

# Quantum Monte Carlo study of a dominant $s$ -wave pairing symmetry in iron-based superconductors

Tianxing Ma,<sup>1,2</sup> Hai-Qing Lin,<sup>2</sup> and Jiangping Hu<sup>3,4,\*</sup>

<sup>1</sup>*Department of Physics, Beijing Normal University, Beijing 100875, China*

<sup>2</sup>*Beijing Computational Science Research Center, Beijing 100084, China*

<sup>3</sup>*Beijing National Laboratory for Condensed Matter Physics,*

*Institute of Physics, Chinese Academy of Sciences, Beijing 100080, China*

<sup>4</sup>*Department of Physics, Purdue University, West Lafayette, Indiana 47907, USA*

(Dated: August 3, 2018)

We perform a systematic quantum Monte Carlo study of the pairing correlation in the  $S_4$  symmetric microscopic model for iron-based superconductors. It is found that the pairing with an extensive  $s$ -wave symmetry robustly dominates over other pairings at low temperature in reasonable parameter region regardless of the change of Fermi surface topologies. The pairing susceptibility, the effective pairing interaction and the  $(\pi, 0)$  antiferromagnetic (AFM) correlation strongly increase as the on-site Coulomb interaction increases, indicating the importance of the effect of electron-electron correlation. Our non-biased numerical results provide a unified understanding of superconducting mechanism in iron-pnictides and iron-chalcogenides and demonstrate that the superconductivity is driven by strong electron-electron correlation effects.

A today's major challenge in the study of iron-based superconductors[1–4] is how to obtain an unified microscopic understanding of the different families of these materials, in particular, iron-pnictides and iron-chalcogenides, which distinguish themselves from each other with distinct Fermi surface topologies[5–7]. In the past several years, the majority of the theoretical studies of iron-based high temperature superconductors were based on models with complicated multi-d orbital band structures[8–18]. The conclusions from these studies provided a good understanding of iron-pnictides while drawing a very different picture regarding of the magnetism and superconductivity of iron-chalcogenides because of their strong dependence on theoretical approximations and the topology of Fermi surfaces. Effective models emphasizing local AFM exchange couplings appear to unify the understanding of superconducting states of both materials[19–27]. However, they lack of a support from more fundamental microscopic electronic physics, and using some unbiased numerical techniques is believed to be the only opportunity to win this great challenge as Hartree-Fock type approaches are biased if the electronic correlation dominates in the system.

Recently, it has been shown that the underlining electronic structure in iron-based superconductors, which is responsible for superconductivity at low energy, is essentially governed by a two-orbital model with a  $S_4$  symmetry, the symmetry of the building block-the trilayer FeAs or FeSe structure in iron-based superconductors. In the model, the dynamics of two  $S_4$  iso-spin components are weakly coupled so that the essential physics is controlled by a single  $S_4$  iso-spin component. Thus, a minimum effective model that captures the low energy electronic and magnetic properties can be well described by an extended one-orbital Hubbard model near half-filling[28]. Such a microscopic understanding provides a new oppor-

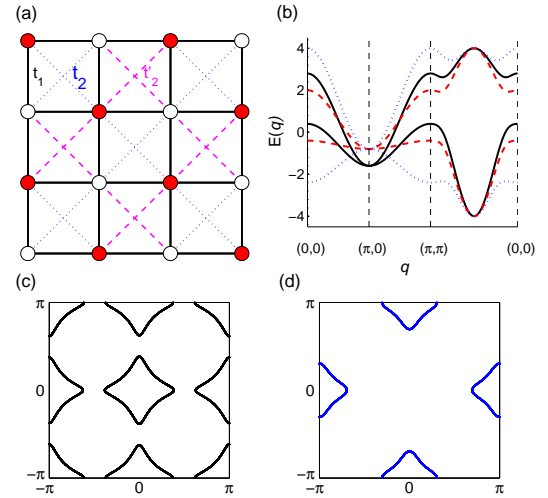


FIG. 1: (Color online)(a) Here red and white circles indicate different sub-lattice A and B. The dark solid lines indicate  $t_1$ , dot blue lines indicates  $t_2$ , and dash purple lines indicates  $t'_2$ . (b) The energy band along high symmetry line in unfolded Brillouin Zone. Solid dark line:  $t_1=0.3$ ,  $t_2=1.4$ ,  $t'_2=-0.6$ ; dash red line:  $t_1=0.3$ ,  $t_2=1.2$ ,  $t'_2=-0.8$  and dot blue line:  $t_1=0.8$ ,  $t_2=1.2$ ,  $t'_2=-0.8$ [29]. (c) Fermi surface at half filling for  $t_1 = 0.3$ ,  $t_2 = 1.4$ ,  $t'_2 = -0.6$  (a typical case for iron-pnictides[30–34]), and (d) at electron filling  $\langle n \rangle = 1.1$  for  $t_1 = 0.8$ ,  $t_2 = 1.2$ ,  $t'_2 = -0.8$  (a typical case for iron-chalcogenides[5–7]).

tunity to make use of highly controllable and unbiased numerical methods to study iron-based superconductors, in particular, to obtain a possible unified understanding of iron-pnictides and iron-chalcogenides.

In this Letter, we perform a systematic quantum Monte Carlo study of the pairing correlation in the  $S_4$  symmetric microscopic model. We find that the pairing with an extensive  $A_{1g}$   $s$ -wave symmetry robustly dominates over other pairings at low temperature in

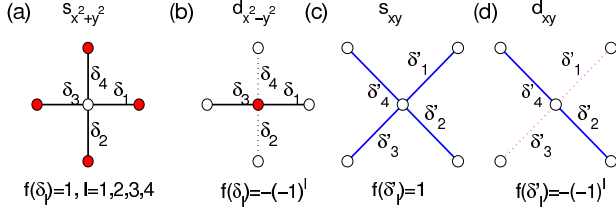


FIG. 2: (Color online) Phase of the  $s_{x^2+y^2}$ ,  $d_{x^2-y^2}$ ,  $s_{xy}$  and  $d_{xy}$ .

reasonable parameter region regardless of the change of Fermi surface topologies, the presence or absence of hole pockets at  $\Gamma$  point. For both iron-pnictides and iron-chalcogenides, the pairing susceptibility, the effective pairing interaction and the  $(\pi, 0)$  AFM correlation strongly increase as the on-site Coulomb interaction increases. Our study demonstrates that the superconductivity in iron-based superconductors is driven by electron-electron correlation and the nesting between electron and hole pockets is not an essential physics in iron-based superconductors. This conclusion is behind many proposed effective models[19–21] but could not be conclusively reached with approximated methods[18]. The fact that the extended  $s$ -wave is favored even in the case without hole pockets differs from the earlier simple conjecture in [11, 12]. Our unbiased numerical results thus present a rather different picture from mean field approaches.

As shown in Fig. 1 (a), the minimum extended Hubbard model for a single  $S_4$  iso-spin component in the iron-square lattice is described by

$$\begin{aligned}
 H = & t_1 \sum_{i\eta\sigma} (a_{i\sigma}^\dagger b_{i+\eta\sigma} + h.c.) \\
 & + t_2 [\sum_{i\sigma} a_{i\sigma}^\dagger a_{i\pm(\hat{x}+\hat{y}),\sigma} + \sum_{i\sigma} b_{i\sigma}^\dagger b_{i\pm(\hat{x}-\hat{y})\sigma}] \\
 & + t_2' [\sum_{i\sigma} a_{i\sigma}^\dagger a_{i\pm(\hat{x}-\hat{y})\sigma} + \sum_{i\sigma} b_{i\sigma}^\dagger b_{i\pm(\hat{x}+\hat{y})\sigma}] \\
 & + U \sum_i (n_{ai\uparrow} n_{ai\downarrow} + n_{bi\uparrow} n_{bi\downarrow}) + \mu \sum_{i\sigma} (n_{ai\sigma} + n_{bi\sigma})
 \end{aligned}
 \quad (1)$$

Here,  $a_{i\sigma}$  ( $a_{i\sigma}^\dagger$ ) annihilates (creates) electrons at site  $\mathbf{R}_i$  with spin  $\sigma$  ( $\sigma=\uparrow, \downarrow$ ) on sublattice A,  $b_{i\sigma}$  ( $b_{i\sigma}^\dagger$ ) annihilates (creates) electrons at the site  $\mathbf{R}_i$  with spin  $\sigma$  ( $\sigma=\uparrow, \downarrow$ ) on sublattice B,  $n_{ai\sigma} = a_{i\sigma}^\dagger a_{i\sigma}$ ,  $n_{bi\sigma} = b_{i\sigma}^\dagger b_{i\sigma}$ ,  $\eta = (\pm\hat{x}, 0)$  and  $(0, \pm\hat{y})$ . In the above model, for simplicity and clarity, we only keep a minimum set of parameters which include three key shortest hopping parameters that are responsible for the physical picture revealed by the  $S_4$  symmetry[28]. The selection of parameters in following studies does capture the essential physics of typical cases for iron-pnictides[30–34] and iron-chalcogenides[5–7], as shown in Fig.1 (b-d).

Our numerical calculations were mainly performed on an  $8^2$  or a  $12^2$  lattice with periodic boundary conditions.

The system was simulated using determinant quantum Monte Carlo (DQMC) at finite temperature. The basic strategy of DQMC is to express the partition function as a high-dimensional integral over a set of random auxiliary fields. The integral is then accomplished by Monte Carlo techniques. In our simulations, 8000 sweeps were used to equilibrate the system. An additional 45000 sweeps were then made, each of which generated a measurement. These measurements were split into fifteen bins which provide the basis of coarse-grain averages and errors were estimated based on standard deviations from the average. For more technique details we refer to Refs. [35–37].

As magnetic excitation might play an important role in the superconducting (SC) mechanism of electronic correlated systems, we first studied the magnetic correlations in such system. We define the spin susceptibility in the  $z$  direction at zero frequency,

$$\chi(q) = \int_0^\beta d\tau \sum_{d,d'=a,b} \sum_{i,j} e^{iq \cdot (i_d - j_{d'})} \langle m_{i_d}(\tau) \cdot m_{j_{d'}}(0) \rangle \quad (2)$$

where  $m_{i_a}(\tau) = e^{H\tau} m_{i_a}(0) e^{-H\tau}$  with  $m_{i_a} = a_{i\uparrow}^\dagger a_{i\uparrow} - a_{i\downarrow}^\dagger a_{i\downarrow}$  and  $m_{i_b} = b_{i\uparrow}^\dagger b_{i\uparrow} - b_{i\downarrow}^\dagger b_{i\downarrow}$ .

To investigate the SC property of iron-based superconductors, we computed the pairing susceptibility,

$$P_\alpha = \frac{1}{N_s} \sum_{i,j} \int_0^\beta d\tau \langle \Delta_\alpha^\dagger(i, \tau) \Delta_\alpha(j, 0) \rangle, \quad (3)$$

where  $\alpha$  stands for the pairing symmetry. Due to the constraint of on-site Hubbard interaction in Eq. (1), pairing between two sublattices is favored and the corresponding order parameter  $\Delta_\alpha^\dagger(i)$  is defined as

$$\Delta_\alpha^\dagger(i) = \sum_l f_\alpha^\dagger(\delta_l) (a_{i\uparrow}^\dagger b_{i+\delta_l\downarrow} - a_{i\downarrow}^\dagger b_{i+\delta_l\uparrow})^\dagger,$$

with  $f_\alpha(\delta_l)$  being the form factor of pairing function. Here, the vectors  $\delta_l$  ( $l=1,2,3,4$ ) denote the nearest neighbour (NN) inter sublattice connections where  $\delta$  is  $(\pm\hat{x}, 0)$  and  $(0, \pm\hat{y})$ , or the next nearest neighbour (NNN) inner sublattice connections where  $\delta'$  is  $\pm(\hat{x}, \hat{y})$  and  $\pm(\hat{x}, -\hat{y})$ .

We study four kinds of pairing form, as that sketched in Fig. 2. For  $s_{x^2+y^2}$ -wave pairing,  $f_s(\delta_l) = 1$ . For  $d_{x^2-y^2}$  pairing,  $f_d(\delta_l)$  is 1 when  $\delta_l = (\pm\hat{x}, 0)$  and -1 otherwise.

Another two interesting pairing forms are  $d_{xy}$ -wave and extensive  $s_{xy}$ -wave,

$$\begin{aligned}
 d_{xy}\text{-wave} : & f_{d_{xy}}(\delta'_l) = 1 (\delta'_l = \pm(\hat{x}, \hat{y})) \\
 \text{and} & f_{d_{xy}}(\delta'_l) = -1 (\delta'_l = \pm(\hat{x}, -\hat{y})), \\
 s_{xy}\text{-wave} : & f_{s_{xy}}(\delta'_l) = 1, \quad l = 1, 2, 3, 4.
 \end{aligned} \quad (4)$$

In Fig. 3, we present the spin susceptibility  $\chi(\mathbf{q})$  at different electron fillings and  $U$  for temperature  $T=1/6$ . A sharp peak at  $(\pi, 0)$  in Fig. 3 indicates the existence of AFM spin correlation in iron-based superconductors

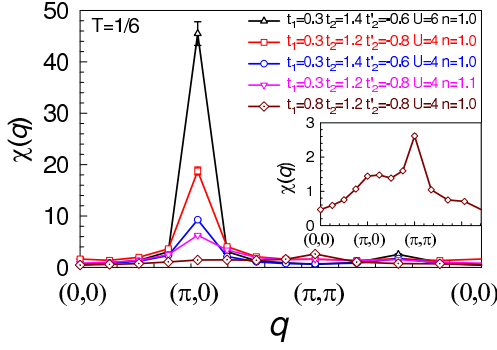


FIG. 3: (Color online) Magnetic susceptibility  $\chi(q)$  versus momentum  $q$  on an  $8^2$  lattice.

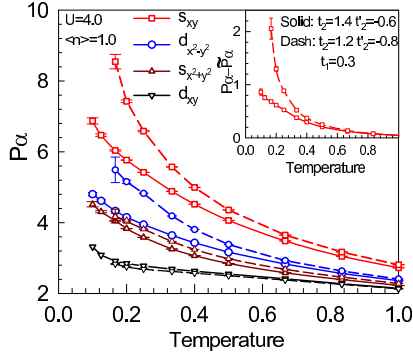


FIG. 4: (Color online) Pairing susceptibility  $P_\alpha$  as a function of temperature for different pairing symmetries at  $t_1 = 0.3, t_2 = 1.4, t'_2 = -0.6$  (solid line) and  $t_1 = 0.3, t_2 = 1.2, t'_2 = -0.8$  (dash line) with  $U = 4.0$  and  $\langle n \rangle = 1.0$  on an  $8^2$  lattice. In the inset: The effective pairing interaction  $P_{s_{xy}} - \tilde{P}_{s_{xy}}$ .

close to half filling. From Fig. 3, one can notice that at half-filling, the peak is very sharp, and as the electron filling  $\langle n \rangle$  decreases from half filling,  $\chi(\mathbf{q})$  is reduced around the  $(\pi, 0)$  point, which indicates that the AFM spin correlation is suppressed when the system is doped away from half filling. The  $(\pi, 0)$  AFM spin fluctuations have been universally observed in all iron-based superconductors[38–44]. It is clear that our model and the results naturally provides an explanation for the stable AFM exchange couplings  $J_2$  observed by neutron scattering[39, 41, 42] in parental compounds.

From the behavior of magnetic correlation shown in Fig. 3, it is also important to note that the  $(\pi, 0)$  spin correlation does not depend on the presence of the hole pockets at  $\Gamma$  point, which indicates that such an AFM correlation is driven by electron-electron correlation rather than nesting between hole and electron Fermi pockets[18]. The  $(\pi, 0)$  AFM correlation is also stabilized by the fact that the diagonal or NNN hopping parameters  $t_2$  are larger than the NN hopping  $t_1$ . As shown in Fig. 3, if  $t_1$  is significantly large, the  $(\pi, \pi)$  magnetic correlation can be dominant. As we will show later, in this case,  $d_{x^2-y^2}$  pairing can be significantly enhanced.

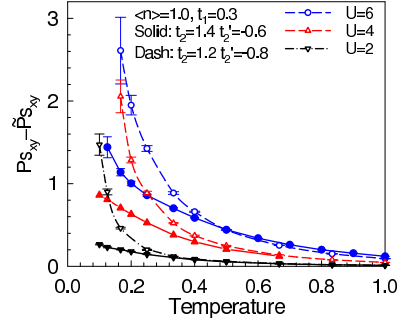


FIG. 5: (Color online) The effective pairing interaction  $P_{s_{xy}} - \tilde{P}_{s_{xy}}$  as a function of temperature for different  $U$  at  $t_1 = 0.3, t_2 = 1.4, t'_2 = -0.6$  (solid line) and  $t_1 = 0.3, t_2 = 1.2, t'_2 = -0.8$  (dash line) on an  $8^2$  lattice.

Fig. 4 shows the temperature dependence of pairing susceptibilities for different pairing symmetries. Within the parameter range investigated, the pairing susceptibilities for various pairing symmetries increase as the temperature is lowered. Most remarkably,  $s_{xy}$  increases much faster than any other pairings symmetry at low temperatures. This demonstrates that the  $s_{xy}$  pairing symmetry is dominant over the other pairing symmetry near half filling. When other parameters are fixed, reducing  $t_{2s} = (t_2 + t'_2)/2$  from 0.4 to 0.2, or increasing the absolute value of  $t'_2$ , one may also see that pairing susceptibilities with different symmetries are all enhanced, in particular, the  $s_{xy}$  pairing susceptibility.

In order to extract the effective pairing interaction in different pairing channels, the bubble contribution  $\tilde{P}_\alpha(i, j)$  is also evaluated, which is achieved by replacing  $\langle a_{i\downarrow}^\dagger b_{j\uparrow} a_{i+\delta_{l\downarrow}}^\dagger b_{j+\delta_{l'\uparrow}} \rangle$  with  $\langle a_{i\downarrow}^\dagger b_{j\uparrow} \rangle \langle a_{i+\delta_{l\downarrow}}^\dagger b_{j+\delta_{l'\uparrow}} \rangle$  in Eq. (3). In the inset of Fig. 4, we plot  $P_{s_{xy}} - \tilde{P}_{s_{xy}}$  for  $t_1 = 0.3, t_2 = 1.4, t'_2 = -0.6$  (solid line). It is apparent that  $P_{s_{xy}} - \tilde{P}_{s_{xy}}$  shows a very similar temperature dependence to that of  $P_{s_{xy}}$ . The effective pairing interaction for  $P_{s_{xy}}$ , is found to take a positive value and to increase with lowering temperature. The positive effective pairing interaction indicates that there actually exists attraction for the  $s_{xy}$  pairing. The effective  $s_{xy}$  pairing interaction for  $t_1 = 0.3, t_2 = 1.2, t'_2 = -0.8$  is also shown in Fig. 4 as dash line. Comparing results with different  $t'_2$ , the effective  $s_{xy}$  pairing interaction is enhanced greatly as the absolute value of  $t'_2$  increases.

In Fig. 5, we present the effective pairing interaction as a function of temperature for  $P_{s_{xy}}$  at different  $U$  with  $t_1 = 0.3, t_2 = 1.4, t'_2 = -0.6$  (solid line) and (b)  $t_1 = 0.3, t_2 = 1.2, t'_2 = -0.8$  (dash line). One can see that, the effective pairing interaction is enhanced as  $U$  increases. Especially, the effective  $s_{xy}$  pairing interaction shown in Fig. 5 tends to diverge in low temperatures, and the increasing  $U$  tends to promote such diverge. This demonstrates that the electron-electron correlation plays a key role in driving the superconductivity.

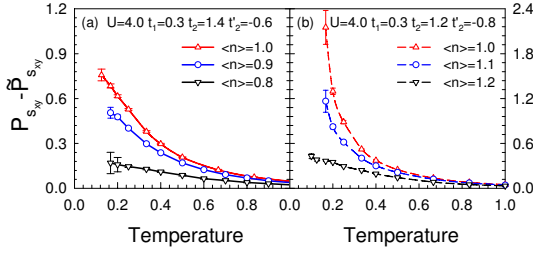


FIG. 6: (Color online) The effective pairing interaction  $P_{s_{xy}} - \bar{P}_{s_{xy}}$  as a function of temperature for different electron fillings at  $t_1 = 0.3, t_2 = 1.4, t'_2 = -0.6$  (solid lines) and  $t_1 = 0.3, t_2 = 1.2, t'_2 = -0.8$  (dash lines) on an  $8^2$  lattice.

We also studied the temperature dependence of effective pairing interaction at different electron fillings. In Fig. 6, the temperature dependence of effective pairing interaction is shown for  $\langle n \rangle = 1.0, 0.9$  and  $0.8$  with  $t_1 = 0.3, t_2 = 1.4, t'_2 = -0.6$  (a); and  $\langle n \rangle = 1.0, 1.1$  and  $1.2$  with  $t_1 = 0.3, t_2 = 1.2, t'_2 = -0.8$  (b). Both Fig. 6 (a) and (b) show that, the effective pairing interaction decreases as the system is doped away from half filling. As shown in Figs. (3,4,6), the decrease of the peak at  $(\pi, 0)$  of spin susceptibility is correlated with the suppression of the pairing susceptibility. This directly confirms that the  $(\pi, 0)$  AFM fluctuations favors the  $s_{xy}$  pairing.

Following, we reported the effect of  $t_1$  on pairing symmetry. In Fig. 7, the pairing behavior for different  $t_1$  is shown for  $\langle n \rangle = 1.1$ . As  $t_1$  increases significantly, it is possible that the  $d_{x^2-y^2}$  wave pairing becomes dominant. A global phase diagram of the leading pairing symmetry in the  $t_1/t_2$ - $|t'_2|/t_2$  plane, obtained by DQMC at temperature  $T = 1/6$ , is shown in the inset of Fig. 7. This phase diagram indicates that the  $s_{xy}$  is robust when  $t_1$  is small. The phase transition line in the inset is roughly corresponding to the hopping parameter setting when the dispersion of the band at  $\Gamma$  which is originally responsible for the hole pocket gets reversed. Since such a reverse does not take place in the band structure of iron-based superconductors[30], the  $s_{xy}$ -wave thus is robust. The robustness is further shown in Fig. 7 where we reported DQMC calculations throughout the  $t_1/t_2$  vs  $t'_2/t_2$  phase diagram. In general, the hopping parameters in the  $S_4$  model is  $t_2 > t_1 > |t'_2|$ , and the fitting to band structure shows that  $t_1$  is roughly  $0.4t_2$  and  $t'_2$  is around  $0.3t_2$ [28].

Finally, we present the pairing susceptibility for different pairing symmetries on a  $12^2$  lattice and compare them to the  $s_{xy}$  pairing susceptibility on an  $8^2$  lattice in Fig. 8. One can see that, the results for a larger lattice size confirm that the  $s_{xy}$  dominates over other kinds of pairing symmetry. Moreover, it is interesting to see that, the  $s_{xy}$  pairing susceptibility increases as the lattice size increases, especially at low temperature. This enhancement is consistent with the behavior of spin susceptibility  $\chi(\mathbf{q})$  shown in the inset of Fig. 8, in which  $\chi(\mathbf{q})$  is also

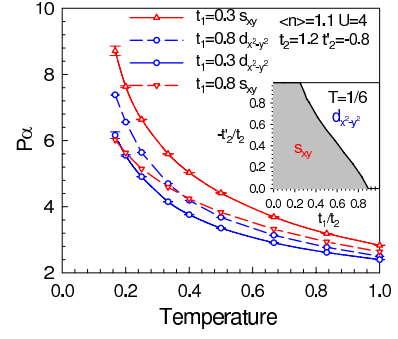


FIG. 7: (Color online)  $P_\alpha$  as a function of temperature at  $\langle n \rangle = 1.1, U = 4.0, t_2 = 1.2, t'_2 = -0.8$  for different  $t_1$  on an  $8^2$  lattice. Inset: the competition between  $s_{xy}$  and  $d_{x^2-y^2}$  depends on  $t_1/t_2$  and  $-t'_2/t_2$ .

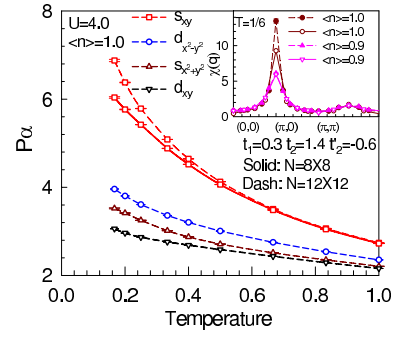


FIG. 8: (Color online)  $P_\alpha$  as a function of temperature for different pairing symmetries at  $t_1 = 0.3, t_2 = 1.4, t'_2 = -0.6$  of a  $12^2$  (dash line) and an  $8^2$  (solid line) lattice with  $U = 4.0$  and  $\langle n \rangle = 1.0$ . In the inset:  $\chi(q)$  versus  $q$  for a  $12^2$  (dash line with solid symbols) and  $8^2$  (solid line with open symbols) lattice at  $\langle n \rangle = 1.0$  (dark red) and  $\langle n \rangle = 0.9$  (pink).

enhanced as the lattice size increases. The peak of  $\chi(\mathbf{q})$  at  $(\pi, 0)$  point increases as the lattice size increases at  $\langle n \rangle = 1.0$ , which implies there may be a static magnetic order develops for the ground state near half filling. The above results of the pairing susceptibility have also shown to be valid when long range pairing correlation are calculated[45]. Thus, the  $8^2$  lattice is large enough to investigate the dominant pairing symmetry.

Overall, these results clearly suggest that the superconductivity and pairing symmetry in iron-based superconductors are determined by the combination of strong electron-electron correlation and the microscopic setting of hopping parameters. In the model, if  $t_2$  and  $t'_2$  are fixed, a small decrease of  $t_1$  can cause the vanishing of hole pockets at  $\Gamma$ . Since the  $d$ -wave pairing channel is caused by  $t_1$ , we can conclude that the  $s$ -wave pairing is ever more robust in iron-chalcogenides than in iron-pnictides, a result completely different from weak coupling approaches. Recent experimental results by angle resolved photoemission spectroscopy have strongly suggested that pairing symmetry in both iron-pnictides[30]



and iron-chalcogenides is a  $s$ -wave[46]. Our study clearly provides such a unified microscopic understanding.

In summary, we study the pairing susceptibility and effective pairing interaction in iron-based superconductors based on an effective  $S_4$  model[28]. It is confirmed that the  $(\pi, 0)$  AFM dominates at half filling and the pairing susceptibility with  $s_{xy}$  symmetry are enhanced as the electron-electron correlation increases, especially at low temperature. It is suggested that the  $s_{xy}$  wave pairing symmetry, which is the  $A_{1g}$  phase corresponding to the point group of the lattice and homogenous with respect to the transitional symmetry of the iron lattice[47], should be dominant in iron-based superconductors. The reported strong AFM at half filling and the behavior of pairing susceptibility and effective pairing interaction strongly support that the microscopic superconducting mechanism for cuprates and iron-based superconductors including both iron-pnictides and iron-chalcogenides are identical.

*Acknowledgement:* JP thanks H. Ding, D.L. Feng for useful discussion. The work is supported by the Ministry of Science and Technology of China 973 program (2011CB922200 and 2012CB821400), NSFCs (Grant. No. 1190024 and No. 11104014), and Research Fund for the Doctoral Program of Higher Education of China 20110003120007.

---

\* Electronic address: jphu@iphy.ac.cn

- [1] Y. Kamihara, T. Watanabe, M. Hirano, and H. Hosono, *J. Am. Chem. Soc.* **130**, 3296 (2008).
- [2] X. H. Chen, T. Wu, G. Wu, R. H. Liu, H. Chen, and D. F. Fang, *Nature* **453**, 761 (2008).
- [3] G. F. Chen et al., *Phys. Rev. Lett.* **100**, 247002, (2008).
- [4] J. Guo et al., *Phys. Rev. B* **82**, 180520 (2010).
- [5] X.-P. Wang, T. Qian, P. Richard, P. Zhang, J. Dong, H.-D. Wang, C.-H. Dong, M.-H. Fang, and H. Ding, *Europhys. Lett.* **93**, 57001 (2011).
- [6] Y. Zhang, L. X. Yang, M. Xu, Z. R. Ye, F. Chen, C. He, H. C. Xu, J. Jiang, B. P. Xie, J. J. Ying, et al., *Nature Materials* **10**, 273 (2011).
- [7] D. Mou, S. Liu, X. Jia, J. He, Y. Peng, L. Zhao, L. Yu, G. Liu, S. He, X. Dong, et al., *Phys. Rev. Lett.* **106**, 107001 (2011).
- [8] P. J. Hirschfeld, M. M. Korshunov, and I. I. Mazin, *arXiv:1106.3712* (2011).
- [9] D. Johnston, *Advances in Physics* **59**, 803 (2010).
- [10] J. Dong, H. J. Zhang, G. Xu, Z. Li, G. Li, W. Z. Hu, D. Wu, G. F. Chen, X. Dai, J. L. Luo, et al., *Europhys. Lett.* **83**, 27006 (2008).
- [11] I. I. Mazin, D. J. Singh, M. D. Johannes, and M. H. Du, *Phys. Rev. Lett.* **101**, 057003 (2008).
- [12] K. Kuroki et al., *Phys. Rev. Lett.* **101**, 087004 (2008).
- [13] F. Wang, H. Zhai, Y. Ran, A. Vishwanath, and D.-H. Lee, *Phys. Rev. Lett.* **102**, 047005 (2009).
- [14] R. Thomale, C. Platt, J. P. Hu, C. Honerkamp, and B. A. Bernevig, *Phys. Rev. B* **80**, 180505 (2009).
- [15] R. Thomale, C. Platt, W. Hanke, J. Hu, and B. A. Bernevig, *Phys. Rev. Lett.* **107**, 117001 (2011).
- [16] A. V. Chubukov, D. V. Efremov, and I. Eremin, *Phys. Rev. B* **78**, 134512 (2008).
- [17] V. Cvetkovic and Z. Tesanovic, *Phys. Rev. B* **80**, 024512 (2009).
- [18] R. Arita, and H. Ikeda, *J. Phys. Soc. Jpn* **78**, 113707 (2009).
- [19] S. Maiti, M. M. Korshunov, T. A. Maier, P. J. Hirschfeld, and A. V. Chubukov, *Phys. Rev. B* **84**, 224505 (2011).
- [20] K. J. Seo, B. A. Bernevig, and J. P. Hu, *Phys. Rev. Lett.* **101**, 206404 (2008).
- [21] Q. Si and E. Abrahams, *Phys. Rev. Lett.* **101**, 076401 (2008).
- [22] C. Fang, H. Yao, W. F. Tsai, J. P. Hu, and S. A. Kivelson, *Phys. Rev. B* **77**, 224509 (2008).
- [23] F. Ma, Z.-Y. Lu, and T. Xiang, *Phys. Rev. B* **78**, 224517 (2008).
- [24] J. Hu and H. Ding, *Scientific Reports* **2**, 381 (2012).
- [25] J. Hu, B. Xu, W. Liu, N. Hao, and Y. Wang, *Phys. Rev. B* **85**, 144403 (2012).
- [26] X. Lu, C. Fang, W.-F. Tsai, Y. Jiang, and J. Hu, *Phys. Rev. B* **85**, 054505 (2012).
- [27] E. Berg, S. A. Kivelson, and D. J. Scalapino, *Phys. Rev. B* **81**, 172504 (2010).
- [28] J. Hu and N. Hao, *Phys. Rev. X* **2**, 021009 (2012).
- [29] The signs of  $t_1$  being the same in the  $x$ - and  $y$ -direction suggests the orbital character of the model can not be pure  $d_{xz}$  and  $d_{yz}$  orbitals. The orbitals in the  $S_4$  model are heavily dressed by the  $d_{xy}$  orbital, and the Wannier functions for the two orbitals of the  $S_4$  model shall be reported in our further work.
- [30] H. Ding et al., *Europhys. Lett.* **83**, 47001 (2008).
- [31] P. Richard et al., *Reports on Progress in Physics* **74**, 124512 (2011).
- [32] L. X. Yang et al., *Phys. Rev. B* **82**, 104519 (2010).
- [33] D. H. Lu et al., *Physica C: Superconductivity* **469**, 452 (2009).
- [34] F. Chen et al., *Phys. Rev. B* **81**, 14526 (2010).
- [35] R. Blankenbecler, D. Scalapino, and R. L. Sugar, *Phys. Rev. D* **24**, 2278 (1981).
- [36] T. Ma, F. M. Hu, Z. B. Huang, and H. Q. Lin, *Appl. Phys. Lett.* **97**, 112504 (2010).
- [37] T. Ma, F. M. Hu, Z. B. Huang, and H. Q. Lin, *Horizons in World Physics*. **276**, Chapter 8, Nova Science Publishers, Inc., (2011).
- [38] C. de La Cruz et al., *Nature* **453**, 899 (2008).
- [39] J. Zhao et al., *Nature Physics* **5**, 555 (2009).
- [40] J. Zhao, H. Cao, E. Bourret-Courchesne, D.-H. Lee, and R. Birgeneau, *arXiv:1205.5992* (2012).
- [41] O. J. Lipscombe et al., *Phys. Rev. Lett.* **106**, 057004 (2011).
- [42] M. Wang et al., *Nature Comm.* **2**, 580 (2011).
- [43] M. Wang et al., *arXiv:1201.3348* (2012).
- [44] J. Hu, B. Xu, W. Liu, N.-N. Hao, and Y. Wang, *Phys. Rev. B* **85**, 144403 (2012).
- [45] T. Ma, H. Q. Lin, J. P. Hu, in preparation.
- [46] X.-P. Wang et al., *arXiv:1205.0996* (2012); M. Xu et al., *arXiv:1205.0787* (2012).
- [47] This is not obvious in the present paper since only one  $S_4$  isospin is considered. However, one can draw this conclusion by considering the parity requirement for spin singlet pairing.